

University of Groningen

Cosmological 21cm experiments

Jelic, Vibor

IMPORTANT NOTE: You are advised to consult the publisher's version (publisher's PDF) if you wish to cite from it. Please check the document version below.

Document Version

Publisher's PDF, also known as Version of record

Publication date:
2010

[Link to publication in University of Groningen/UMCG research database](#)

Citation for published version (APA):

Jelic, V. (2010). *Cosmological 21cm experiments: searching for a needle in a haystack*. [Thesis fully internal (DIV), University of Groningen]. University of Groningen.

Copyright

Other than for strictly personal use, it is not permitted to download or to forward/distribute the text or part of it without the consent of the author(s) and/or copyright holder(s), unless the work is under an open content license (like Creative Commons).

The publication may also be distributed here under the terms of Article 25fa of the Dutch Copyright Act, indicated by the "Taverne" license. More information can be found on the University of Groningen website: <https://www.rug.nl/library/open-access/self-archiving-pure/taverne-amendment>.

Take-down policy

If you believe that this document breaches copyright please contact us providing details, and we will remove access to the work immediately and investigate your claim.

Downloaded from the University of Groningen/UMCG research database (Pure): <http://www.rug.nl/research/portal>. For technical reasons the number of authors shown on this cover page is limited to 10 maximum.

Chapter 1

Scientific rationale

About four hundred million years after the birth of our Universe the first objects were formed, which then started to ionize the surrounding gas with their strong radiation. Six hundred million years later, the all-pervasive gas was transformed from a neutral to an ionized state. This pivotal period in the history of the Universe is called the Epoch of Reionization (EoR). It holds the key to structure formation and evolution, but also represents a missing piece of the puzzle in our current knowledge of the Universe. Currently, this is changing with the completion of a new generation of radio telescopes, which are capable of directly probing the EoR. LOFAR is the first telescope of this kind, and will use an array of simple radio antennas to hunt for the radiation emitted by the neutral hydrogen during the EoR. The wavelength of this radiation is 21 cm, but on its way to us it is stretched by the Universe's expansion to the radio wavelengths of 1–2 m. However, its detection will be quite a challenge due to a number of complicating factors. For example, the desired signal is so weak that it is like *a needle in a haystack*, overwhelmed by the prominent foreground emission of our own Galaxy and other extragalactic radio sources. This thesis examines both the properties of the "haystack" and the way it influences the LOFAR-EoR experiment, and discusses the Cosmic Microwave Background radiation (the oldest radiation in the Universe) as an additional probe of the EoR.

In this introductory chapter we first take a fly through the history of the Universe and we place the EoR on the Universe's time (Sec. 1.1). Then, we give a brief overview on the CMB radiation (Sec. 1.2). Section 1.3 explains observational constraints of the EoR and introduces its new observational probe: the redshifted 21 cm line. The main scientific goals and challenges of the LOFAR-EoR experiment are presented in Sec. 1.4. The chapter concludes with an overview and the major goals of this thesis (Sec. 1.5).

1.1 Fly through a history of the Universe

It is broadly accepted that the Universe was born 13.7 billion years ago in an event called the Big Bang (BB). The Universe was in a hot dense state and since then it has expanded and evolved into the vast and much cooler cosmos we currently live in. In the following few paragraphs we will take a fly through a history of the Universe (see Fig. 1.1).

During the Planck time, 10^{-43} s after the BB, the Universe is homogeneous, isotropic

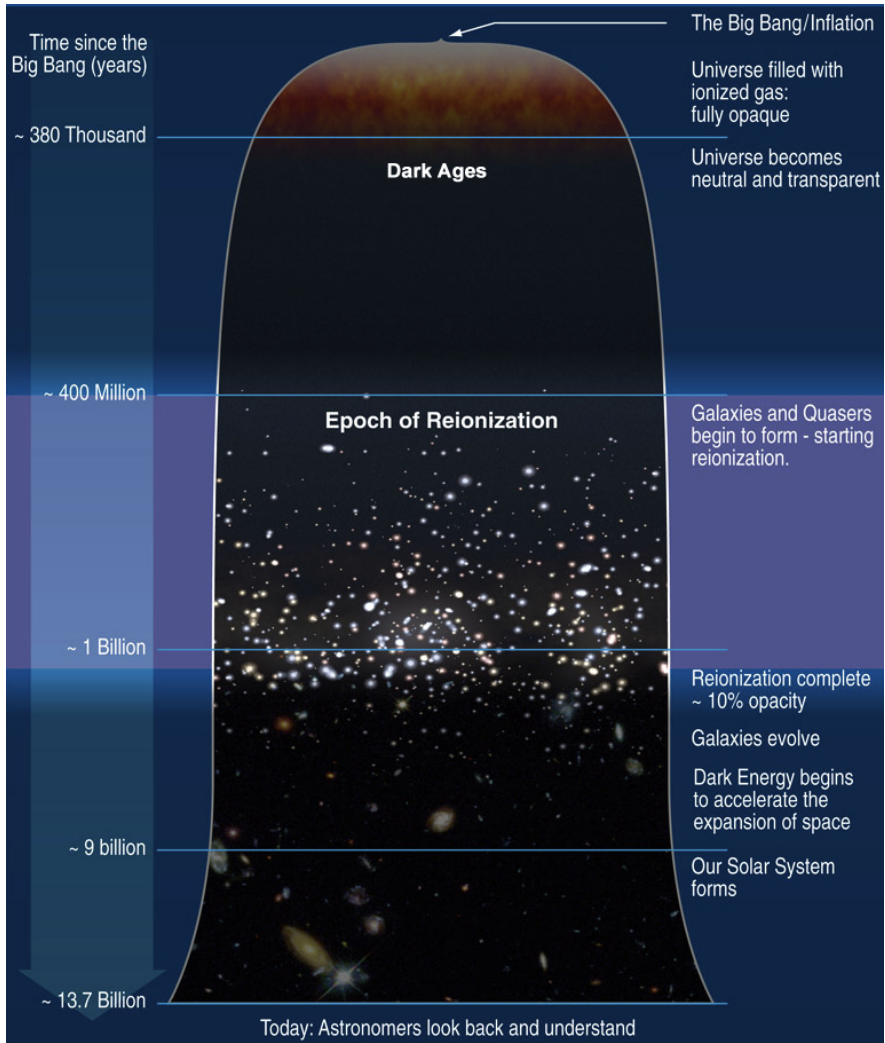


Figure 1.1: A timeline of the Universe with the Epoch of Reionization marked. (Courtesy of WMAP/NASA Scientific Team)

and in a hot, dense and quantum state. A moment later, the size of the Universe increases by a factor of $\sim 10^{26}$ via a rapid and exponential expansion, namely inflation. Soon after, the matter annihilates with the antimatter in a process called baryogenesis. Since there is asymmetry between baryons and anti-baryons, only matter survives. The Universe is almost 10^{-3} s old, expands and cools down.

One second after the BB, the Universe is filled with a sea of neutrons, protons, electrons, anti-electrons (positrons), photons, and neutrinos and its temperature is $\sim 10^{10}$ K. As the Universe continues to cool, the neutrons either decayed into protons or combine with protons to make deuterium (an isotope of hydrogen). During the first three minutes of the Universe, most of the deuterium combines to make helium. This process of light element formation via fusion in the early Universe is called primordial nucleosynthesis. A small amount of lithium is also produced at this time.

Since the Universe is still hot and full of electrons, protons, and light nuclei, the photons easily scatter off the electrons. Thus, the Universe is fully opaque, but this scattering produces a thermal (blackbody) spectrum of radiation. One month after the BB, the expansion of the Universe becomes faster than the scattering process and the blackbody spectrum of the Universe is fixed. Moreover, it will preserve its spectrum information to the present time.

Eventually 380 000 years after the BB, the Universe has cooled sufficiently that protons and electrons can combine to form neutral hydrogen, during the process called recombination. At this point, the rate of combination of an electron and proton to form neutral hydrogen is higher than the ionization rate of hydrogen.

The final result of recombination and primordial nucleosynthesis is that about 3/4 of the baryonic matter is hydrogen and 1/4 is helium. Immediately afterwards, as photons interact barely with the neutral hydrogen, radiation decouples from the baryons and the Universe becomes transparent. The relic radiation from that moment is known as the Cosmic Microwave Background (CMB) radiation. It has a black body spectrum and today is redshifted to the microwave part of the spectrum.

The Universe enters into the period of darkness, known as the Universe's Dark Ages, as there are no radiation sources other than the gradually darkening cosmic background radiation. During the Dark Ages, in high density regions, matter collapses and forms the first stars, black holes, etc. about 400 million years after the BB. These first objects start to emit radiation that ionizes the surrounding material, mostly hydrogen. The Dark Ages are over and the new epoch starts: the Epoch of Reionization (EoR). EoR lasts for the next 600 million years and during this period the cosmic gas changes from being almost completely neutral to almost completely ionized.

During and after the EoR, the structures in the Universe continue to evolve. The first stars explode and spread heavier elements (e.g. carbon, nitrogen, oxygen, silicon, magnesium and iron) in the intergalactic medium (IGM). These heavier elements act as a catalyst for new born stars and provide them with a long lifetime. Bit by bit, stars and gas merge together and they form galaxies, while groups of galaxies form clusters.

Around 9.1 billion years after the BB, our Sun and the Solar System are formed. On the planet Earth life starts to evolve. It took about 3.5 billion years of evolution to form mammals and additionally a hundred million years to develop from the early mammals to us. At the present time, 13.7 billion years after the Big Bang, scientists are putting effort to understand the Universe that we live in.

Now let's have a more closer look at the Epoch of Reionization and its two observational probes: the Cosmic Microwave Background radiation and the redshifted 21 cm line.

1.2 Cosmic Microwave Background radiation

The Cosmic Microwave Background radiation is the oldest light in the Universe. The study of its properties enable us to make fundamental measurements of cosmology and constrain our Universe: its age, curvature, energy-matter content and evolution.

It also plays an important role for understanding of the EoR. Thus, in the subsections that follow, we give an overview of the discovery of the CMB, present its properties and the physical processes that shape its fluctuations. Its secondary fluctuations are discussed with a special care, since they directly constrain the EoR and could be used as an independent probe of the EoR. The latter is one of the two main topics of this thesis and it is discussed in Ch. 6.

1.2.1 Overview

The Cosmic Microwave Background radiation was predicted by R. Alpher, R. Herman, and G. Gamow in their work on the Big Bang nucleosynthesis (Gamow, 1946; Alpher & Herman, 1949). Some sixteen years later, A. Penzias and R. Wilson made the first observation of this radiation, but their discovery was unintentional (Penzias & Wilson, 1965). They had been working at Bell Telephone Laboratories on a radiometer, which was intended to be used for satellite communication experiments. The instrument was showing an unexplained excess noise above the antenna temperature which was independent on the direction of the antenna towards the sky. Coincidentally, researchers at Princeton University were designing an experiment to find the CMB. When they heard about the Bell Labs result they immediately realized that the CMB had been found (Dicke et al., 1965). In 1978, Penzias and Wilson got the Nobel prize in physics for their discovery.

Further research on the CMB revealed that the CMB was expected to be largely isotropic, but in order to explain the large scale structures observed today, small anisotropies should exist. These anisotropies were discovered by the Cosmic Background Explorer (COBE) and later confirmed by the Wilkinson Microwave Anisotropy Probe. The results obtained from the COBE data provided for the first time evidence that supported the Big Bang theory of the Universe: the CMB has a near perfect black-body spectrum and has very faint anisotropies. Thus, two of COBE's principal investigators, G. Smoot and J. Mather, received the Nobel Prize in Physics in 2006 for their work on the project. According to the Nobel Prize committee, "the COBE-project can also be regarded as the starting point for cosmology as a precision science".

Today, the temperature of the CMB radiation is very low, only 2.7 K. This radiation shines primarily in the microwave part of the electromagnetic spectrum. In fact, the temperature of this radiation is astonishingly uniform in every direction, to better than one part in a thousand. However, there are small temperature isotropies with a root mean square (*rms*) of only $\sim 20 \mu\text{K}$. These anisotropies can be divided into two categories: the primary and secondary anisotropies.

The primary CMB anisotropies originate from the last scattering surface ($z \sim 1100$) and arise due to effects at the time of recombination. There are three basic mechanisms

that generate the primary anisotropies:

1. Sachs-Wolfe (SW) effect: photons from high density regions have to climb out of potential wells, and are thus gravitationally redshifted (Sachs & Wolfe, 1967);
2. Intrinsic adiabatic effect: the coupling of matter and radiation in high density regions can compress radiation and raise its temperature (Peebles & Yu, 1970);
3. Doppler effect: the plasma has a non-zero velocity, which leads to the Doppler shift of the CMB photons (Sunyaev & Zeldovich, 1970).

The first effect is on the large scales, while the other two are on the small scales. In addition to these effects there is also a photon diffusion damping – the process of diffusing photons and equalizing the temperatures of hot and cold regions – which suppresses CMB anisotropies at the smallest angular scales (Silk, 1967).

The secondary CMB anisotropies are generated after the Universe’s recombination by scattering along the way towards us. By studying the detailed physical properties of the primary and secondary CMB anisotropies we can learn about the content of the Universe, its primordial density fluctuations that seeded large-scale structure formation, and the Universe’s further evolution. A more detailed description of the secondary anisotropies is given in the following subsection.

1.2.2 Secondary anisotropies

The CMB photons observed today have traveled a great distance through the Universe from the last scattering surface to us. On their way they have interacted with matter along their path and these interactions generated the secondary anisotropies. There are two major types of interactions: due to gravity and due to scattering of the CMB photons on free electrons. The gravity effects on the CMB photons are:

1. The *integrated Sachs-Wolfe (ISW) effect* is also caused by gravitational redshift, similarly to the primary SW effect. However, we distinguish two different types of this effect. First, the early type ISW effect that occurs immediately after the primary SW effect while the Universe is still dominated in its density by radiation. Second, the late type ISW effect that occurs in recent cosmic history, as dark energy starts to dominate and govern the Universe’s expansion. Note that the ISW effect assumes a linear time-varying gravitational potential. The ISW is also a large scale effect.
2. The *Rees-Sciama effect* is a late type ISW effect but which assumes a non-linear time-varying gravitational potential, usually associated with gravitational collapse. The relevant scales are those of clusters and superclusters (5–10 arcmin).
3. *Gravitational lensing* of the CMB by intervening matter, which is only significant on the scales below a few arc minutes.

The scattering effects are as follows.

1. The *thermal Sunyaev-Zel'dovich (tSZ) effect* is the result of the interaction between the CMB photons and a hot plasma through inverse Compton scattering. During the interaction, the low energy photons are boosted to higher energies. There will be fewer photons in the long-wavelength part of the CMB spectrum (Rayleigh-Jeans tail) and more in the short-wavelength part (Wien tail). This effect is on the scale of galaxy clusters and superclusters, although it may be produced on very small scales during the Epoch of Reionization.
2. The *kinetic Sunyaev-Zel'dovich (kSZ) effect* is the Doppler effect due to the bulk motion of electrons that scatter the photons. There are no distortions of the CMB spectrum. Instead the whole spectrum is blue- or red- shifted depending on the velocity direction.
3. The *Ostriker-Vishniac (OV) effect* is the same as the kSZ effect but in a linear regime.

Note that this subsection is based on Aghanim et al. (2008, review). Please refer to it for more details on the secondary CMB anisotropies.

1.3 Epoch of Reionization

About four hundred million years after the Big Bang the first radiation-emitting objects in the Universe formed, and the all-pervasive gas transformed from neutral to ionized. This pivotal era, the Epoch of Reionization, holds the key to structure formation and evolution in the early Universe, and is a central topic in this thesis.

In the subsections that follow, we will present the observational effort to constrain the EoR but also to probe it directly. The physics involved in the EoR will be explained briefly. For a detail theoretical overview we recommend a few recent reviews by Barkana & Loeb (2001); Ciardi & Ferrara (2005) and Furlanetto et al. (2006).

1.3.1 Observational constraints

At present, there are only two tentative observational constraints on the EoR: the Cosmic Microwave Background and the Gunn-Peterson troughs. As we will explain, both of these observations provide strong evidence for the existence of the EoR, but yet limited constraints.

The primary CMB radiation is linearly polarized as a result of Thompson scattering between the CMB photons and free electrons during recombination. However, the CMB photons are then re-scattered for the second time on the free electrons produced during the EoR. This re-scattering of the photons generates a new signature (anisotropy) in the CMB polarization at large angular scales. The size of the polarization anisotropy relates to the size of the horizon at that epoch and thus depends on the redshift. Therefore, each time the CMB photons are scattered at a certain redshift, there will be a signature in polarization at different scales.

In the CMB power spectrum the signature (anisotropy) produced by EoR is seen as a bump. Its location is related to the redshift of reionization, while its height is defined by the integrated optical depth of free electrons produced during EoR. In other words

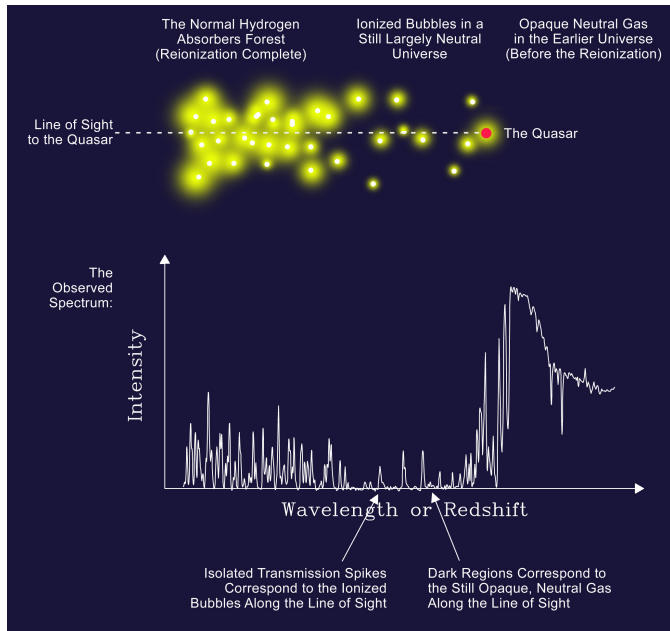


Figure 1.2: An illustration of a quasar spectrum with the Gunn-Peterson trough and $\text{Ly}\alpha$ forest (Courtesy of S. G. Djorgovski et al., Caltech).

the height of the bump is proportional to the duration of reionization. Recently, Dunkley et al. (2009) have used the WMAP Five-Year observations of the CMB to constrain the optical depth of reionization to $\tau = 0.087 \pm 0.017$. Using a simple model for the reionization history, they have found the redshift of reionization to be $z_{\text{reion}} = 11.0 \pm 1.4$. It is important to note that the reionization signature in the polarized CMB data is weak, amounting to no more than 10 percent of the primary signal, and that the redshift constraint is heavily model dependent. Therefore, the CMB constraint on the EoR is limited.

The Gunn-Peterson trough is a feature in a quasar spectrum produced by the neutral hydrogen in the intergalactic medium located between the quasar and the observer. The trough is characterized by the suppression of the quasar emission at wavelengths blue-ward of the quasar $\text{Ly}\alpha$ emission line.

After recombination and until the formation of the first stars, the IGM is opaque and consists of neutral gas. Once the first stars begin to emit radiation that ionizes the surrounding medium, the amount of neutral hydrogen will decrease. However, even a small fraction of neutral hydrogen will make an optical depth of the IGM that is high enough to suppress the observed emission as the scattering cross-section of $\text{Ly}\alpha$ photons with neutral hydrogen is very high. Only after reionization is completed, the density of the neutral hydrogen in the IGM is low enough that it is not capable of suppressing all of the observed emission. Then usually, the quasar spectrum is full of $\text{Ly}\alpha$ absorption lines produced by neutral hydrogen along the line of sight, but at different redshifts (also known as $\text{Ly}\alpha$ forest). An illustration of these features is presented in Fig. 1.2.

A number of authors have analyzed the features in observed quasars spectra and

have drawn the following two conclusions. First, hydrogen in the recent Universe is highly ionized. Second, the neutral fraction of hydrogen in the distant Universe suddenly increases at redshift ~ 6.5 , designating the end of the reionization process. Despite these data providing strong constraints on the ionization state of IGM at redshifts below 6.5, they say very little about the reionization process itself.

1.3.2 New observable of the EoR: Redshifted 21 cm line

The current observations discussed above have been giving us only an estimate on the redshift period of the EoR, but they are not able to give answers to the following three fundamental questions:

- When exactly the reionization had happened?
- What were the first sources that reionized the Universe?
- How reionization had happened?

However, two things are certain: the reionization process had happened and today's Universe is highly ionized. Therefore, there is a need for a dedicated experiment to directly detect the signal from the EoR. The observable that these experiments will use is explained in this subsection.

At the end of the Second World War, Dutch astronomer Hendrik van de Hulst computed the transition frequency of the hyperfine transition line of neutral hydrogen, i.e. ~ 1420 MHz, or equivalent to a wavelength of ~ 21 cm, falling within the radio region of the electromagnetic spectrum. Neutral hydrogen consists of a single proton orbited by a single electron. The proton and electron also have spin, classically analogous to rotational motion of the particle around its axis. The spin of the electron and proton can be in the same direction, i.e. parallel state, and in an opposite direction, i.e. antiparallel state. Because of magnetic interactions between the particles, the parallel state has slightly more energy than the antiparallel state. The effect is also known as hyperfine splitting. During the transition from the parallel to the antiparallel state, a 21 cm photon will be emitted, as a result of energy conservation. Note that the probability of this transition is extremely small, $2.9 \cdot 10^{-15} \text{ s}^{-1}$.

Van de Hulst also predicted that the amount of neutral atomic hydrogen in the interstellar medium would be enough to produce a measurable signal at the radio wavelength of 21 cm. After the 21 cm line was detected by Ewen and Purcell at Harvard University for the first time and was corroborated by Dutch astronomers Muller and Oort at the Leiden Observatory, we can say that van den Hulst's discovery led to a breakthrough in radio astronomy.

A decade later, George Field estimated that neutral hydrogen in the intergalactic medium may also be directly detected via the hydrogen 21 cm line, but in emission or absorption against the cosmic microwave background radiation (CMB) (e.g. Field, 1957, 1959). The physical quantity that measures the 21 cm radiation is the brightness temperature and its derivation follows.

The amount of emission that is radiated by a source is usually expressed in terms of specific intensity, I_ν [$\text{Wm}^{-2}\text{sr}^{-1}\text{Hz}^{-1}$], i.e. energy emitted per unit time per unit area

per solid angle and unit frequency. A black body at temperature T emits radiation at the frequency ν according to Planck's law:

$$I_\nu = \frac{2h}{c^2} \frac{\nu^3}{e^{\frac{h\nu}{k_B T}} - 1}, \quad (1.1)$$

where h is Planck's constant, k_B is Boltzmann's constant and c is the speed of light. In the limit of very high temperatures or small frequencies, Planck's law can be written as the Rayleigh-Jeans law:

$$I_\nu = \frac{2\nu^2}{c^2} \frac{k_B}{T}. \quad (1.2)$$

In radio astronomy, where the limit of small frequencies is applicable, the radiation intensity is usually expressed in terms of temperature (see Eq. 1.2) and it is called a brightness temperature, T_b :

$$T_b(\nu) = \frac{c^2}{2k_b\nu^2} I_\nu. \quad (1.3)$$

Thus T_b is a physical quantity that is measured with the radio telescope. However, as we mentioned before, the 21 cm emission of the IGM can only be detected differentially as a deviation from the CMB and therefore depends on the brightness temperature of the CMB, T_{CMB} , spin temperature, T_s and the density of neutral hydrogen atoms, n_{HI} :

$$\delta T_b \sim n_{\text{HI}} \left(1 - \frac{T_{CMB}}{T_s} \right). \quad (1.4)$$

Note that δT_b is also a function of redshift and the cosmological parameters, but we will come back to this point in the following chapters. The spin temperature quantifies the excitation temperature for the 21 cm transition, i.e. the ratio between the number of neutral hydrogen atoms in parallel and antiparallel hyperfine states:

$$\frac{n_1}{n_0} = \frac{g_1}{g_0} e^{\frac{E_{10}}{k_B T_s}}, \quad (1.5)$$

where $g_{0,1}$ is the statistical weight (here $g_0 = 1$ and $g_1 = 3$), $E_{10} = 5.9 \cdot 10^{-6}$ eV is the energy difference between the states and often E_{10}/k_b is expressed as the equivalent temperature $T_\star = 0.068$ K.

At the end of the 20th century, Madau et al. (1997) first showed that δT_b of the 21 cm emission could provide a direct probe of the Epoch of Reionization. From Eq. 1.4 one can see that there are three possible regimes of the 21 cm detection: if $T_s \gg T_{CMB}$, then the 21 cm radiation is detected as emission; if $T_s \ll T_{CMB}$, then 21 cm radiation is detected as absorption; and if $T_s = T_{CMB}$, there is no 21 cm detection. Thus, to be able to detect the cosmological 21 cm emission, T_s and T_{CMB} need to be decoupled.

Field himself showed that the spin temperature is determined by the three competing processes: absorption of CMB photons; collisions between the particles, which is defined by the gas kinetic temperature, T_k ; and scattering of ambient UV ($\text{Ly}\alpha$) photons, which are defined via temperature, T_α , (Field, 1958):

$$T_s = \frac{T_{CMB} + y_k T_k + y_\alpha T_\alpha}{1 + y_k + y_\alpha}. \quad (1.6)$$

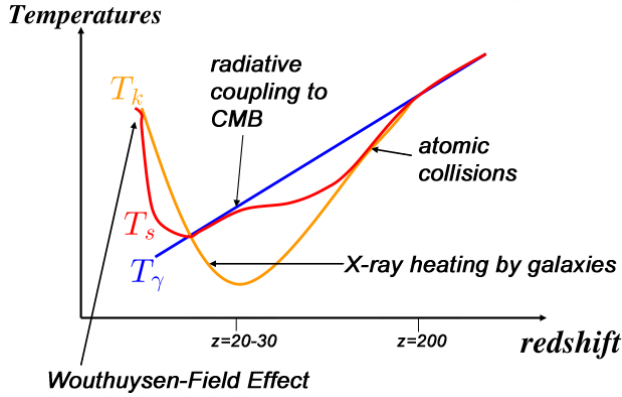


Figure 1.3: “Schematic sketch of the evolution of the kinetic temperature, T_k , and spin temperature, T_s , of cosmic hydrogen. Following cosmological recombination at $z \sim 10^3$, the gas temperature (orange curve) tracks the CMB temperature (blue line; $T_\gamma \propto (1+z)$) down to $z \sim 200$ and then declines below it ($T_k \propto (1+z)^2$) until the first X-ray sources (accreting black holes or exploding supernovae) heat it up well above the CMB temperature. The spin temperature of the 21cm transition (red curve) interpolates between the gas and CMB temperatures. Initially it tracks the gas temperature through collisional coupling; then it tracks the CMB through radiative coupling; and eventually it tracks the gas temperature once again after the production of a cosmic background of UV photons... Parts of the curve are exaggerated for pedagogic purposes. The exact shape depends on astrophysical details...” (fig. 58, Loeb, 2006).

Coupling coefficients for the collision and Ly α terms are y_k and y_α , but for most cases one can assume that $T_\alpha = T_k$. The Ly α coupling term is actually due to the Lyman- α pumping mechanism – also known as the Wouthuysen-Field effect – the hydrogen atom changes hyperfine state through the absorption and spontaneous re-emission of a Ly α photon.

Therefore, T_s and T_{CMB} could be decoupled through either collisions, Lyman-alpha pumping or a combination of both. Which one will happen during the EoR depends also on the type of ionization sources. For example, stars decouple the spin temperature mainly through radiative Ly α pumping while mini-quasars decouple it through a combination of collisional Ly α pumping and heating. An example of the evolution of cosmic hydrogen via its T_s and T_k is shown in Fig. 1.3. However, the important point is that T_s and T_{CMB} are decoupled.

1.3.3 EoR experiments

The 21 cm emission line from the EoR is redshifted by the expansion of the Universe to meter wavelengths. For example, the 21 cm photon emitted at a redshift of 9 has today a wavelength of 2.1 m, or equivalently, a frequency of ~ 140 MHz. Thus, the observation of 21 cm radiation from the EoR requires a radio telescope that operates in a low radio part of the frequency spectrum (100 – 200 MHz). All of the current radio telescopes lack enough sensitivity in these frequencies. Fortunately, during this year this should change with the start-up of two novel radio telescopes: the Low Frequency Array (LOFAR) and

the Murchison Widefield Array (MWA). Both of these have the specific goal to observe the cosmological 21 cm line from the EoR. LOFAR¹ is European effort led by the Netherlands, while the MWA² is built by Australia and the US. There are also a number of other EoR projects: EoR with the Giant Metrewave Telescope³, the 21 Centimeter Array⁴ and the Precision Array to Probe the EoR⁵. By far the most ambitious project is Square Kilometer Array⁶ (SKA), which has an international character and will be build within a decade.

As we will see in the next section, through the LOFAR-Epoch of Reionization key science project, observations of the redshifted 21 cm line will not be easy due to a number of complicating factors. Despite these difficulties, the near future will be very exciting for this field as observational success will open a completely new area in cosmology, shedding light on the Universe's Dark Ages and the Epoch of Reionization.

1.4 LOFAR-EoR key science project

The LOFAR-EoR experiment is a key science project of the LOFAR telescope and it is designed to detect the redshifted 21 cm line of neutral hydrogen from the Epoch of Reionization. In the following three subsections, we will give a technical and scientific overview of the LOFAR project and the LOFAR-EoR key science project will be presented through its scientific goals and challenges. For additional information we refer to the LOFAR and LOFAR-EoR websites (www.lofar.org and www.astro.rug.nl/~LofarEoR), and a project plan of the LOFAR-EoR key science project (de Bruyn, Zaroubi & Koopmans, 2007).

1.4.1 Overview

LOFAR is a new and innovative telescope that will observe at low radio frequencies, the lowest energy extreme of the spectrum that is accessible from Earth. The LOFAR telescope consists of many sensors (dipole antennae) that work together as one big telescope, i.e. interferometric aperture synthesis array. The innovative aspect of LOFAR is its pointing system that is not mechanical. Instead, the LOFAR antennae detect the radiation from the whole observable sky at the same time, and then pointing towards a certain direction is done electronically. This enables observations at the same time in multiple directions and makes LOFAR an IT (Information Technology) telescope. LOFAR is being developed by a consortium of knowledge institutes, universities and industrial parties in Europe, led by Netherlands Institute for Radio Astronomy, ASTRON.

There are two distinct LOFAR antenna types: the Low Band Antenna (LBA) and the High Band Antenna (HBA). LBAs are sensitive in the frequency range between 10 and 80 MHz and consist of simple dual polarization droop dipoles above a conducting ground plane with the wires at an angle of 45 degrees with respect to the ground (see Fig. 1.4). The field of view of an LBA extends to the horizon. HBAs are sensitive in the frequency range between 120 to 240 MHz. They are assemblies (tiles) of 16 bow-tie shaped dual

¹<http://www.lofar.org>

²www.mwatelescope.org

³<http://gmrt.ncra.tifr.res.in>

⁴<http://21cma.bao.ac.cn>

⁵<http://astro.berkeley.edu/~dbacker/eor>

⁶<http://www.skatelescope.org>

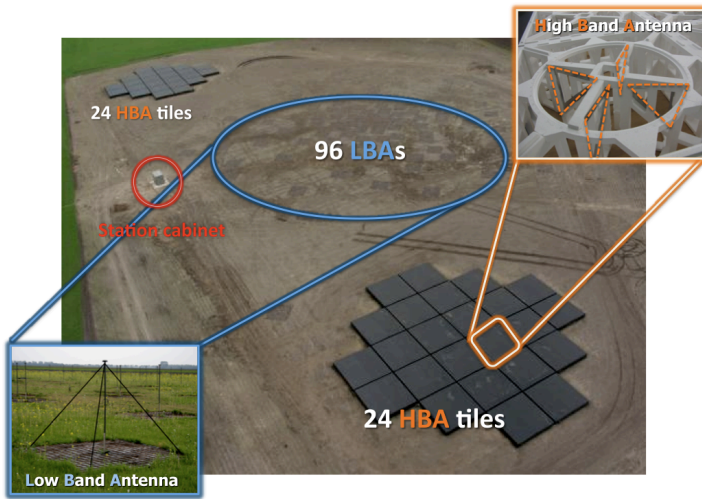


Figure 1.4: An example of a LOFAR core station, which consists of 96 Low Band Antennae (LBAs) and 2×24 High Band Antenna (HBA) tiles organized in a “Micky Mouse” shape.

dipole antennae arranged in a 4×4 grid (see Fig. 1.4). Each HBA tile is designed to have the field of view of ≈ 30 degrees at a frequency of 150 MHz.

The LBA and HBA sensors are organized in array stations. Currently, 36 array stations are being constructed in the North-East of the Netherlands: half of the stations, i.e. 18 core stations, are located in a 2×3 kilometer core area around the village of Exloo and the remaining stations, i.e. 18 remote stations, are distributed around the core at distances up to 80 km (see Fig. 1.5). Each core station consists of 96 LBAs and 2×24 HBA tiles organized in a “Micky Mouse” shape, while a remote station has 96 LBAs and all 48 HBA tiles organized in a single group. In the middle of the core area, 6 core stations are organized in a circle and act as the “super station”. There are also several international stations that are being built in Germany, Sweden, the UK and France.

Since the station fields are distributed over a region of roughly a hundred kilometers in diameter in the Netherlands and up to thousands of kilometers across Europe, for coherent data processing it is necessary to combine the signals from all of the stations with the wide area network. This network then transports the output data streams from the stations to the Central Processing Facility (CEP) in Groningen, the Netherlands. CEP is divided in three sections: an on-line section for processing real-time data streams from the stations, a storage section for collecting the processed data streams and the off-line processing section for additional data analysis. The 1.5 Blue Gene/P supercomputer is used for on-line processing with a power of 34 TFlops.

Due to LOFAR’s cutting-edge technological approach, LOFAR will open an entirely new window on the Universe at frequencies of $\sim 10 - 240$ MHz (corresponding to wavelengths of 1.2 – 30 m). It will provide a broad range of astrophysical studies with unprecedented resolution and will make a breakthrough in sensitivity that can lead to unexpected “serendipitous” discoveries, i.e., the detection of new classes of objects and new astrophys-



Figure 1.5: An approximate location of the LOFAR core area (red circle) and remote stations (blue circles). The data from the stations is processed in Groningen with a Blue Gene supercomputer.

ical phenomena. Currently, there are six major scientific studies, i.e. key science projects, designed to pursue fundamental LOFAR science.

- **EPOCH OF REIONIZATION** – LOFAR will search for the signals from neutral hydrogen, when the Universe was only ~ 400 Myr old and when the radiation of the first sources started to (re)ionize the surrounding gas, mostly neutral hydrogen;
- **DEEP EXTRAGALACTIC SURVEYS** – LOFAR will explore the formation of the earliest structures in the Universe, i.e. galaxies, clusters and black holes, and will detect a zoo of various distant massive radio galaxies;
- **TRANSIENT SOURCES** – LOFAR will detect very short flashes of radiation, coming from exploding stellar giants, accreting supermassive black holes and rapidly rotating superdense neutron stars;
- **ULTRA HIGH ENERGY COSMIC RAYS** – LOFAR will detect radiation from the ultra high energy cosmic rays as they pierce the Earth's atmosphere;
- **SOLAR SCIENCE AND SPACE WEATHER** – LOFAR will monitor the solar activity and its effect on the Earth, observe coronal mass ejections from the Sun and map the ionospheric disturbances caused by the solar wind;
- **COSMIC MAGNETISM** – LOFAR will map magnetic fields in our own and nearby galaxies, in galaxy clusters and the intergalactic medium.

In addition to the astrophysical applications, the LOFAR wide field network will be also used for geophysical and agricultural applications. Therefore, LOFAR is a real multiple sensor array that uses common infrastructure, data transport, power and processing capabilities for multidisciplinary research.

1.4.2 Scientific goals

The main goals of the LOFAR-EoR key science project are the detection and quantification of the cosmological 21 cm signal from the EoR. The former should be achievable in the first years of observations, while the later demands higher signal to noise and should be achieved during the succeeding years.

A detailed list of the main scientific goals of the LOFAR-EoR project follows.

1. *Statistical detection of the ionization history of the Universe as a function of redshift:* The measured δT_b of the cosmological 21 cm signal is mainly dependent on the number of neutral hydrogen atoms at a certain redshift. Thus, by measuring the variance of the cosmological 21 cm signal at the resolution scale of LOFAR, i.e., $\langle \delta T_b^2 \rangle - \langle \delta T_b \rangle^2$, we can determine a global reionization history. Using the LOFAR-EoR simulation pipeline, Jelić et al. (2008) have demonstrated this type of statistical detection of the EoR signal (see Ch. 5).
2. *Power spectrum of the underlying density fluctuations:* According to the current models of the EoR, LOFAR will be able to probe the intergalactic medium prior to significant reionization and obtain the power spectrum of the underlying cosmological density field (Harker et al., *in prep.*). Note that this could be achieved only if the spin temperature of the intergalactic medium is much higher than the CMB temperature.
3. *Higher order statistics of the EoR signal:* There is a lot of information in the signal that is not contained in the power spectrum. Therefore, it is important to analyze the cosmological 21 cm signal with high order statistical measures, such as skewness, kurtosis, bi-spectrum, Minkowski functionals, etc (e.g. Harker et al., 2009b).
4. *Statistical characterization of the growth of the size of the ionized regions as a function of redshift:* Since ionized regions will not contribute to the observed signal below the scale of their typical size, the power spectrum of the measured 21 cm brightness temperature as a function of redshift will provide information about this issue.
5. *Study of individual ionization bubbles around high redshift ionization sources:* The bubbles around a supermassive black hole or cluster of the first stars might have a radius larger than a resolution element of the LOFAR-EoR experiment. Studying such bubbles and their spatial structure will enable us to study the nature of the ionization sources.
6. *21 cm forest:* The radiation emanating from a strong high redshift radio source could be absorbed by the neutral hydrogen intervening along the line of sight (Carilli et al., 2002). Such absorption would then produce a forest of 21 cm absorption lines just like the one produced by the Lyman α transition in the spectrum of lower redshift

quasars. This type of measurement would provide a direct tomography of the neutral hydrogen along the line of sight. However, note that the statistics of such sources is very poorly known and might be quite rare.

7. *Cross-correlation studies:* Data obtained during the LOFAR-EoR experiment can be combined with some other astrophysical observations. The main rationale is that other astrophysical data might (anti-)correlate with the EoR signal. Two main types of data in mind are given below.

- (a) *CMB data:* The kinetic Sunyaev-Zel'dovich effect – produced by the scattering of CMB photons off free electrons produced during the reionization process – and the cosmological 21 cm signal – which reflects the neutral hydrogen content of the Universe, as a function of redshift – might cross-correlate at the certain scales (see Ch. 6). Given the recent launch of the PLANCK satellite, which has measured the CMB with unprecedented accuracy, it is fit to conduct a rigorous study into the cross-correlation of these data sets.
- (b) *Catalogues of galaxies at high- z :* Since galaxies harbor the sources of ionization, they are expected to anti-correlate with the EoR signal. Recent study have shown that the LOFAR-EoR experiment could be sensitive to the 21 cm–galaxy cross spectrum in conjunction with the Subaru survey of Lyman-alpha emitters (Lidz et al., 2009).

Beside the primary goals, the LOFAR-EoR experiment will provide the deepest images of the sky in the low radio part of the spectrum. These observations can be used then for additional (namely secondary) scientific studies:

1. *The physics of Galactic emission processes:* Combined deep images of the radio sky obtained for the LOFAR-EoR experiment with additional follow up studies at 20 – 80 MHz can be used to explore the physics that govern Galactic emission processes, constrain the properties of the regular and random component of the Galactic magnetic fields and distribution of the cosmic ray and thermal electrons.
2. *Tomographic ionospheric studies:* A detail statistical characterization of the ionosphere is needed in order to detect the weak cosmological 21 cm signal. Therefore, the obtained ionospheric phase fluctuations on scales of arc minutes to degrees and time-scales of seconds to hours can be used for tomographic studies of the ionosphere.
3. *Deep long-baselines studies of foreground sources:* Deep long-baseline studies of the foreground sources will provide a catalogue of faint supernovae remnants, radio clusters and galaxies that will be of interest on its own.
4. *Faint transients:* Very long and deep integrations of the LOFAR-EoR observations will detect many faint transient sources.

1.4.3 Challenges

The LOFAR-EoR experiment, as well as other experiments designed to measure the cosmological 21 cm line, are challenged by strong astrophysical foreground contamination,

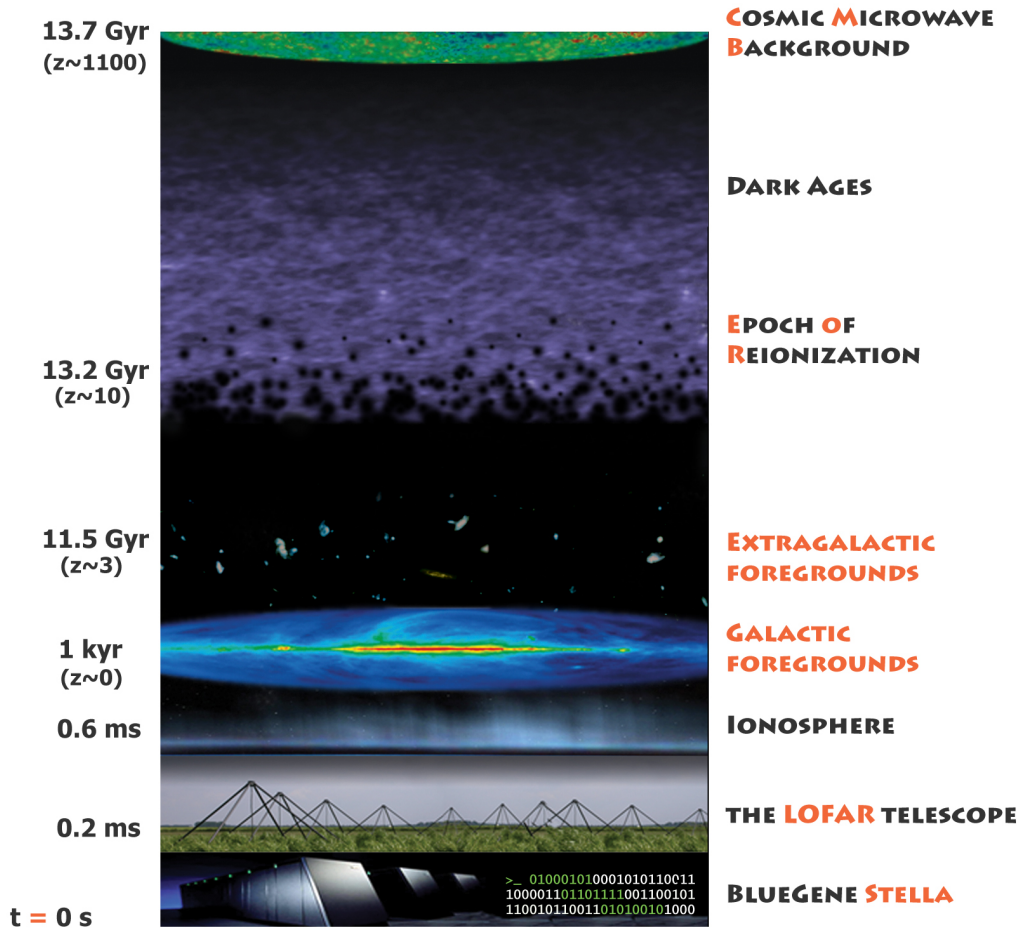


Figure 1.6: This sketch illustrates all contributions to and contaminations of the observed signal in the case of the LOFAR-EoR key science project. The former are: Galactic foregrounds $\sim 71\%$, extragalactic foregrounds $\sim 27\%$, CMB $< 1\%$ and the EoR signal $\sim 0.01\%$; and the latter are: ionosphere, radio frequency interferences, and instrumental effects and noise. On the left, a travel time of the observed signal is noted.

ionospheric distortions, complex instrumental response and other different types of noise (see Fig. 1.6). In the following few paragraphs we will give a brief description of each.

In the frequency range of the EoR experiments ($\sim 100 - 200$ MHz) the foreground emission of our own Galaxy and extragalactic sources (radio galaxies and clusters) dominate the sky. In fact, the amplitude of this foreground emission is 4–5 orders of magnitude stronger than the expected cosmological 21 cm signal. However, since the radio telescopes, which are used for the EoR observations, are interferometers, they measure only fluctuations of a signal. The ratio between the foregrounds and the cosmological signal is reduced to 2 – 3 orders of magnitude.

In terms of physics, the foreground emission originates mostly from the interaction between relativistic charged particles and a magnetic field, i.e. synchrotron radiation. Galactic synchrotron radiation is the most prominent foreground emission and contributes about 70% to the total emission at 150 MHz (Shaver et al., 1999). The contribution from the extragalactic synchrotron radiation is $\sim 27\%$, while the smallest contribution ($\sim 1\%$) is from Galactic free-free emission, i.e. thermal radiation of an ionized gas.

Ionospheric distortions of the signal detected by a radio telescope are caused by variations in the total electron content of the upper most part of the atmosphere, i.e. the ionosphere, which is ionized by solar radiation. Thus, multiple scattering of an incoming radio wave on electrons in the ionosphere produces scintillation of the observed source and makes its image blurred. However, these effects can be removed to a certain degree by a process called ionospheric calibration.

Any interferometric radio telescope has a complex instrumental response, which introduces artifacts in an observed image and significantly contaminates the signal. Moreover, the instrument itself introduces noise in an observation in terms of the brightness of the sky and the system temperature. Hopefully, the artifacts introduced by the instrumental response can be removed through calibration of the instrument, while the noise can be beaten down by sufficiently long integrations.

The last type of contamination in the EoR experiments is Radio Frequency Interference (RFI). RFI is a disturbance due to either electromagnetic conduction or electromagnetic radiation emitted from an external source, e.g. radio and television emitters, communication devices etc. Luckily, in most cases they are narrow banded and tend to occur at the same position in time and frequency. Their properties can be studied in detail and excised accurately.

Given all of the challenges that need to be overcome in order to reliably detect the EoR signal, it is crucial to understand all of their properties and characteristics. Thus, the LOFAR-EoR experiment end-to-end simulation is developed in order to study the effect of these contaminants on the detection of the cosmological signal.

1.5 This thesis

In the previous sections, we have seen the importance of exploring the Epoch of Reionization, a missing puzzle in the process of structure formation and evolution in the Universe. We have seen numerous efforts to probe this epoch using radio interferometric telescopes that are designed to detect the 21 cm line of neutral hydrogen from the redshifts of EoR. We have also seen the challenges that these experiments need to overcome in order to

reliably detect the cosmological 21 cm signal: prominent foreground emission, complex ionospheric distortions and instrumental response, radio frequency interferences and different types of noise. If not treated and removed correctly, all of these challenges could severely contaminate the EoR signal and obstruct its detection. Therefore, the hunt for the cosmological 21cm signal can be truly compared with *finding the needle in the haystack*.

However, in the last decade there has been a slew of theoretical and observational efforts to explore and understand all of the data components of the EoR experiments in order to prepare us for the real data. Thus, the ultimate effort is an end-to-end simulation of the EoR experiment, which will help us to develop a robust signal extraction scheme for the extremely challenging EoR observations. In addition, it will help us to understand very well all of the data components, their influence on the desired signal and explore additional complementary or corroborating probes of the EoR.

This thesis focuses on the LOFAR-EoR key science project. More precisely on two aspects of the project:

1. *Foreground simulations as part of the LOFAR-EoR simulation pipeline;*
2. *The cosmic microwave background as an additional probe of the EoR.*

In the following few paragraphs we will give a brief description of each.

1. The LOFAR-EoR simulation pipeline consists of three main modules: the EoR signal (described in the thesis by R. M. Thomas, 2009), the foregrounds (this thesis) and the instrumental response (described in the thesis by P. Labropoulos, *in prep.*). Additional modules are: the ionosphere (described in the thesis by P. Labropoulos, *in prep.*), the radio frequency interferences (described in the thesis by A. Offringa, *in prep.*), the inversion (described in the thesis by P. Labropoulos, *in prep.*) and different extraction schemes (Jelić et al., 2008; Harker et al., 2009a,b). A flow chart of all of these modules is shown in Fig. 1.7.

The LOFAR-EoR foreground model, presented in this thesis, contains all of the foreground components both in total and polarized intensity: Galactic synchrotron emission from diffuse and localized sources, Galactic thermal (free-free) emission and integrated emission from extragalactic sources, like radio galaxies and clusters. The Galactic emission is simulated with special care to include all its physical properties and characteristics. It is important to note that a developed foreground model is the first model to simulate the EoR foregrounds in great detail.

2. One of the leading sources of secondary anisotropy in the CMB is due to the scattering of CMB photons off free electrons created during the reionization process. These anisotropies can be induced by thermal motions of free electrons (thermal Sunyaev-Zel'dovich effect) and by the bulk motion of free electrons (the kinetic Sunyaev-Zel'dovich effect, kSZ). The latter is far more dominant during reionization. Therefore, it is useful to consider the mutual information that the CMB and the cosmological 21cm data sets contain. Along these lines, in this thesis we have obtained a cross-correlation study between the kSZ effect – produced by the scattering of CMB photons off free electrons produced during the reionization process – and the cosmological 21 cm signal – which reflects the neutral hydrogen content of the Universe, as a function of redshift.

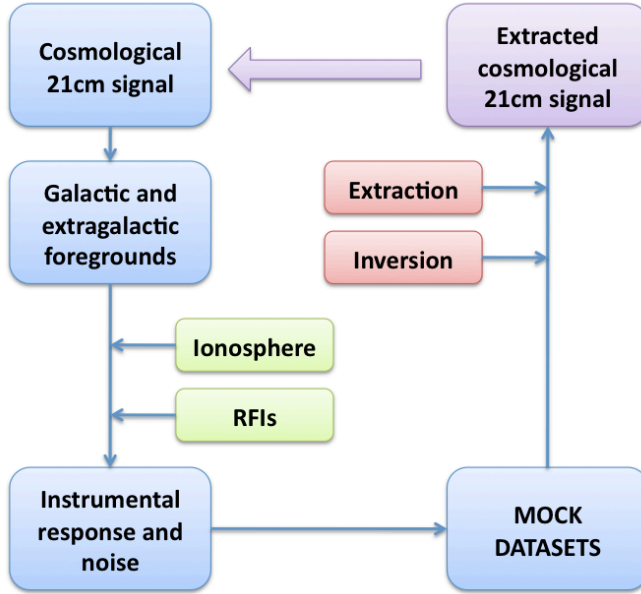


Figure 1.7: A flow chart of the LOFAR-EoR simulation pipeline, which will help us to develop a robust signal extraction scheme for the extremely challenging EoR observations.

Summa summarum, this thesis has the following aims:

- To provide a detailed foreground model for the LOFAR-EoR simulation pipeline that includes both galactic and extragalactic emission. The model has to be capable of simulating the foreground maps tailored in the angular and frequency domains for the LOFAR telescope.
- To study the properties of the Galactic diffuse synchrotron emission in total and polarized intensity using both simulations and current observations.
- To explore the influence of the total and polarized intensity foregrounds on extraction schemes for the cosmological 21cm signal.
- To investigate the kSZ-21cm cross-correlation as an additional probe of the EoR.

This thesis is organized as follows. The galactic and extragalactic foreground simulations tailored for the LOFAR-EoR experiment are presented in Ch. 2. A detail Galactic synchrotron emission model for total and polarized intensities is presented in Ch. 3. Chapter 4 shows the results on simulated Galactic synchrotron emission in the region of Abel 2255. The effect of the total and polarized intensity foregrounds on the extraction of the EoR signal is explained in Ch. 5. Chapter 6 discusses the cross-correlation study between the cosmological 21cm signal and CMB data. The thesis finishes with the final remarks (Ch. 7).

